Spring 5-26-1960

Core Location of Extensive Air Showers

James H. Jett

CORE LOCATION OF EXTENSIVE AIR SHOWERS - JETT

CORE LOCATION OF
EXTENSIVE AIR SHOWERS

By

James H. Jett

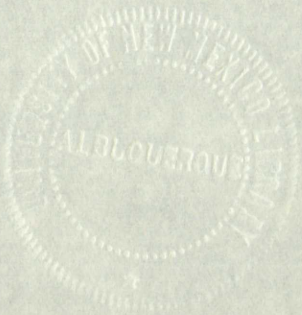

A Thesis

Submitted in Partial Fulfillment of the

Requirements for the Degree of

Master of Science in Physics

The University of New Mexico

1961

This thesis, directed and approved by the candidate's committee, has been accepted by the Graduate Committee of the University of New Mexico in partial fulfillment of the requirements for the degree of

MASTER OF SCIENCE

E. L. Castetter
Dean

May 26, 1961
Date

CORE LOCATION OF EXTENSIVE AIR SHOWERS

by

James H. Jett

Thesis committee

John R. Green
Chairman

Roy Thomas

Victor H. Regener

TABLE OF CONTENTS

LIST OF TABLES

LIST OF ILLUSTRATIONS

PART I. CORE LOCATION OF EXTENSIVE AIR SHOWERS

1. Introduction

Extensive air showers have been studied as a part of cosmic ray phenomenology since 1938.[1] They are made up of electrons, photons and many other particles which traverse the earth's atmosphere toward the earth. The showers are initiated by high energy primary cosmic rays. The primary cosmic rays are nuclei which have been stripped of their orbital electrons. Most of the primaries are protons and deuterons; the rest of the primaries are nuclei of higher atomic number. Table 1 gives the percent of the total number of primary cosmic rays for various values of atomic number z.

TABLE I

COMPOSITION OF THE PRIMARY COSMIC RAYS[2]

z	Percent of Total
1	77
2	21
3-5	0.1
6-10	1.6
> 10	.3

When a high energy primary penetrates the nucleus of an atom the primary interacts with the nucleons near its path. This interaction of the primary with the nucleons of the nucleus releases several pi-mesons, the struck nucleons, and possibly other strange particles and antinucleons.[2]

PART I. CORE LOCATION OF EXTENSIVE AIR SHOWERS

1. Introduction

Extensive air showers have been studied as a part of cosmic ray phenomenology since 1938.[1] They are made up of electrons, protons and many other particles which traverse the earth's atmosphere before reaching earth. The showers are initiated by high energy primary cosmic rays. The primary cosmic rays are nuclei which have been stripped of their orbital electrons. Most of the primaries are protons and deuterons; the rest of the primaries are nuclei of higher atomic number. Table 1 gives the percent of the total number of primary cosmic rays for various values of atomic number Z.

TABLE 1

COMPOSITION OF THE PRIMARY COSMIC RAYS[2]

Z	Percent of Total
1	72
2	21
3-5	0.1
6-10	1.6
> 10	.3

When a high energy primary penetrates the nucleus of an atom the primary interacts with the nucleons over its path. This interaction of the primary with the nucleons ejects nucleons from the struck nucleus, the struck nucleons, and sometimes other strange particles and antinucleons.[3]

The primary usually continues on after suffering a loss of energy and possibly some deflection from its original path during the interaction. The high energy pi-mesons, which were produced in the collision, are contained in a small cone around the path of the primary after the collision. The liberated nucleons form a larger cone, in the forward direction, around the path of the primary. The primary and the nucleons which have sufficient energy continue on to give more collisions with nuclei in the atmosphere. The pi-mesons decay into photons and mu-mesons; the latter in turn decay into electrons.

These high energy electrons and photons give rise to the soft component of the extensive air shower. When an electron is accelerated by the strong electric field of a nucleus, it can emit a gamma ray; the electron continues on after it has been deflected. This process is called bremsstrahlung. The photons undergo pair production. By this process a photon, when it is in the field of a nucleus, "materializes" into an electron-positron pair. Pair production and bremsstrahlung are the two main processes by which the soft component of the air shower is enlarged. By the time the shower reaches the surface the soft component along with the mu-mesons has spread out laterally up to several hundred meters from the axis of the shower.

On the way through the atmosphere the particles produced in the electron-photon cascade lose energy through their radiative interactions and through ionization of the atmosphere. When the average energy of the electrons and photons falls below a certain level (84.2 MeV) the shower stops growing in terms of number of particles and begins to die off. It is known that energy must be transferred from the core of the shower, the

region containing the high energy particles, to the more widespread electron-photon cascade. A measure of the transfer of energy from the core of the shower to the electronic component of the shower is what is desired.

To this end an experiment is under way in the University of New Mexico Physics Department to determine the amount of energy transferred from the core of the shower to the electron-photon cascade. By using a detector telescope with appropriate absorber between the two detectors, the amount of energy transferred can be determined. To do this work it is necessary to know where the core of the shower is located relative to the detector telescope system and how large the shower is in terms of the total number of particles in the shower. The first part of this thesis deals with a practical method of locating the axis of the shower.

2. Principle of Triangulation and Geometry

When an extensive air shower strikes the surface of the earth five variables must be specified to completely describe the shower. Two of these are angles which define the direction the shower came from, i.e., the axis of the primary. In this work the deviation from the normal can be ignored since most of the showers strike nearly normal to the surface of the earth.[3] Two variables specify the location of the core of the shower. Last, the size of the shower must be specified.

The experimental set-up consists of five scintillation detectors. Two of them form a vertical telescope. They are 10 ft. in diameter. The three other scintillators are smaller (3 ft. in diameter) and are arranged in the form of an isosceles triangle with the telescope system mid-way between. Figure 1 shows the set-up with the appropriate dimensions.

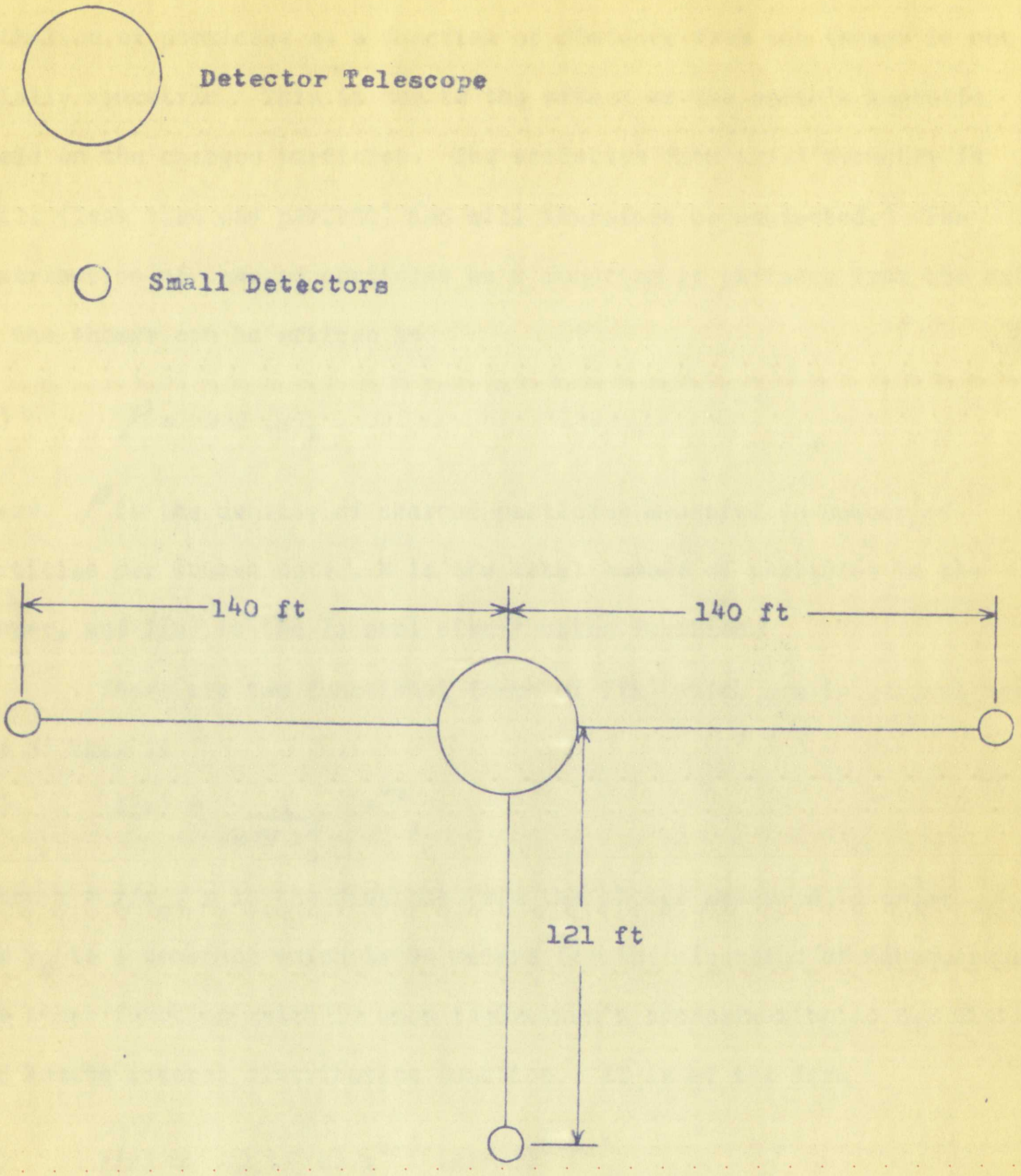

FIGURE 1

LOCATION OF DETECTORS

When an air shower reaches the surface of the earth, the distribution of particles as a function of distance from the shower is not axially symmetric. This is due to the effect of the earth's magnetic field on the charged particles. The variation from axial symmetry is small (less than one percent) and will therefore be neglected.[1] The distribution of charged particles as a function of distance from the axis of the shower can be written as

$$(1) \qquad \rho = N f(x),$$

where ρ is the density of charged particles measured in number of particles per square meter, N is the total number of particles in the shower, and f(x) is the lateral distribution function.

There are two functional forms of f(x) which are in general use. One of them is

$$(2) \qquad f(x) = \frac{1}{2\pi r_o^2} \frac{e^{-x}}{x},$$

where $x = r/r_o$, r is the distance from the shower measured in meters, and r_o is a constant which is 94 meters for the elevation of Albuquerque.[3,4] The other function which is used is Greisen's approximation to the Nishimura and Kamata lateral distribution function. It is of the form

$$(3) \qquad f(x) = \frac{1}{r_4^2} C(s)\, x^{s-2} (x+1)^{s-4.5},$$

where $x = r/r_4$; $r_4 = 97$ meters for Albuquerque; C(s) is a normalization factor; and s is the age parameter.[5] For this part of the work the exponential function will be used. It is very close to Greisen's function for the area of main interest. The merits and demerits of the various distribution functions have been discussed by Barton.[6]

When an air shower reaches the earth, the distribution of particles as a function of distance from the core is not axially symmetric. This is due to the effect of the earth's magnetic field on the charged particles. The variation from axial symmetry is small (less than one percent) and will therefore be neglected.[7] The distribution of charged particles as a function of distance from the axis of the shower can be written as

$$\rho = N\, f(x) \qquad (1)$$

where ρ is the density of charged particles measured in number of particles per square meter, N is the total number of particles in the shower, and f(x) is the lateral distribution function.

There are two functional forms of f(x) which are in general use. One of them is

$$f(x) = \frac{1}{2\pi r_o^2}\, e^{-x} \qquad (2)$$

where $x = r/r_o$, r is the distance from the shower axis measured in meters, and r_o is a constant which is 94 meters for the elevation of Albuquerque. The other function which is used is Greisen's approximation to the Nishimura and Kamata lateral distribution function. It is of the form

$$f(x) = \frac{1}{r_1^2}\, C(s)\, x^{s-2}\,(x+1)^{s-4.5} \qquad (3)$$

where $x = r/r_1$, $r_1 = 97$ meters for Albuquerque; C(s) is a normalization factor; and s is the age parameter.[8] For this part of the work the exponential function will be used. It is very close to Greisen's and is used for the area of main interest. The merits and demerits of the various distribution functions have been discussed by Burton.[9]

The co-ordinate used is indicated in Figure 2. From the drawing the following relationships, which will be used later, can be derived relating R, θ, r_1, r_2, and r_3 as defined by the drawing.

(4) $$r_1^2 = R^2 + b^2 - 2RbSin\theta$$

$$r_2^2 = R^2 + a^2 - 2RaCos\theta$$

$$r_3^2 = R^2 + a^2 - 2RaCos\theta$$

The scintillator at each location determines the number of particles traversing it. The area A of these detectors is 0.656 square meters. Thus, if N_i is the number of particles traversing the i^{th} tank, then the density of particles at the location of that tank is given by

(5) $$\rho_i = N_i/A \ .$$

This equation neglects the variation of the density of particles over the area of the tank. Now there are three pieces of data, i.e., the densities ρ_1, ρ_2, and ρ_3. The quantities R, θ, and N are to be determined. R and θ give the location of the shower axis relative to the large scintillators and N gives the total number of particles in the shower. Thus the problem is just one of solving three equations in three unknowns.

3. Method of Solution

The three equations to be solved are

(6) $$\rho_1 = \frac{N}{2\pi r_o^2} \frac{e^{-x_1}}{x_1} \ ,$$

$$\rho_2 = \frac{N}{2\pi r_o^2} \frac{e^{-x_2}}{x^2} \ ,$$

and $$\rho_3 = \frac{N}{2\pi r_o^2} \frac{e^{-x_3}}{x^3} \ .$$

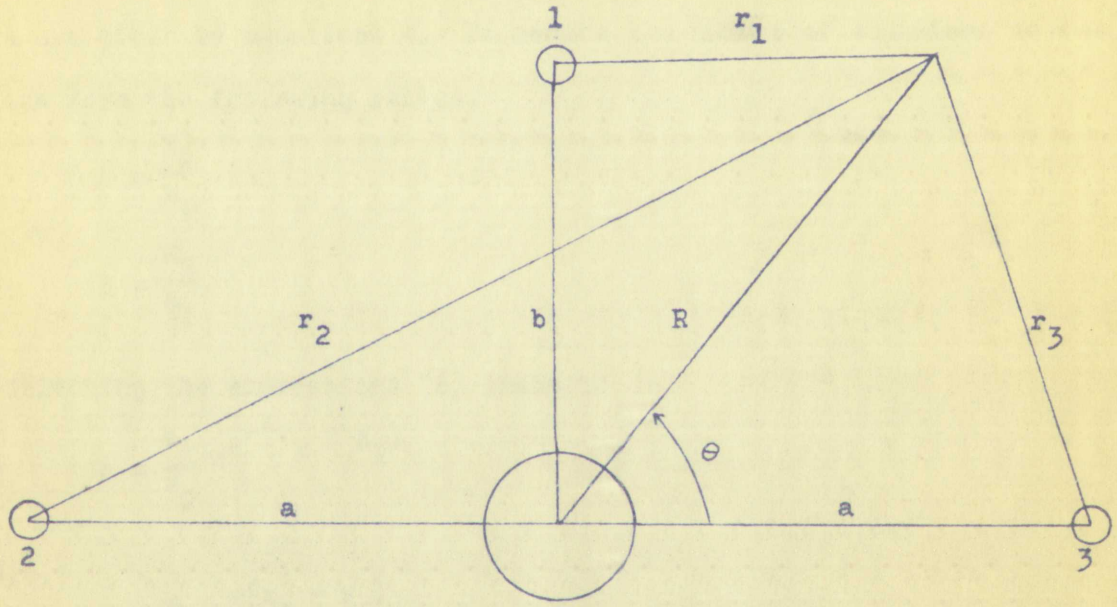

Detector Telescope

Small Detectors

FIGURE 2

CO-ORDINATE SYSTEM

where $x_1 = r_1/r_o$, etc. These equations can be written directly in terms of the number of particles traversing the tank as

$$(7) \qquad N_i = \frac{NA}{2\pi r_o^2} \frac{e^{-x_i}}{x_i} .$$

The relationships between the x_i and the co-ordinates (R, θ) of the shower core are given by equations 4. To reduce the number of equations to two, we can form the following ratios.

$$(8) \qquad A = \frac{N_2}{N_1}$$

$$B = \frac{N_3}{N_1}$$

Substituting the expressions (6) leads to

$$(9) \qquad A = \frac{x_1}{x_2} e^{-(x_2 - x_1)}$$

and,

$$(10) \qquad B = \frac{x_1}{x_3} e^{-(x_3 - x_1)} .$$

These equations have only two unknowns in them. They are R and θ.

From this point on, one can use two practical methods of finding the simultaneous solution to these equations. One method is to use a computer and by an iterative method find the best solution for each set of data points. The other method is to find the solution of the equations graphically. The latter method is the one which will be discussed here. Let lines of R vs. θ be plotted for constant r_i in accordance with equations 4. Figure 3 shows two sets of these lines. The lines shown are lines of constant r_1 and r_2. These lines of constant r_i are also lines of constant $F(x_i)$, where,

$$(11) \qquad F(x_i) = \frac{1}{x_i} e^{-x_i} .$$

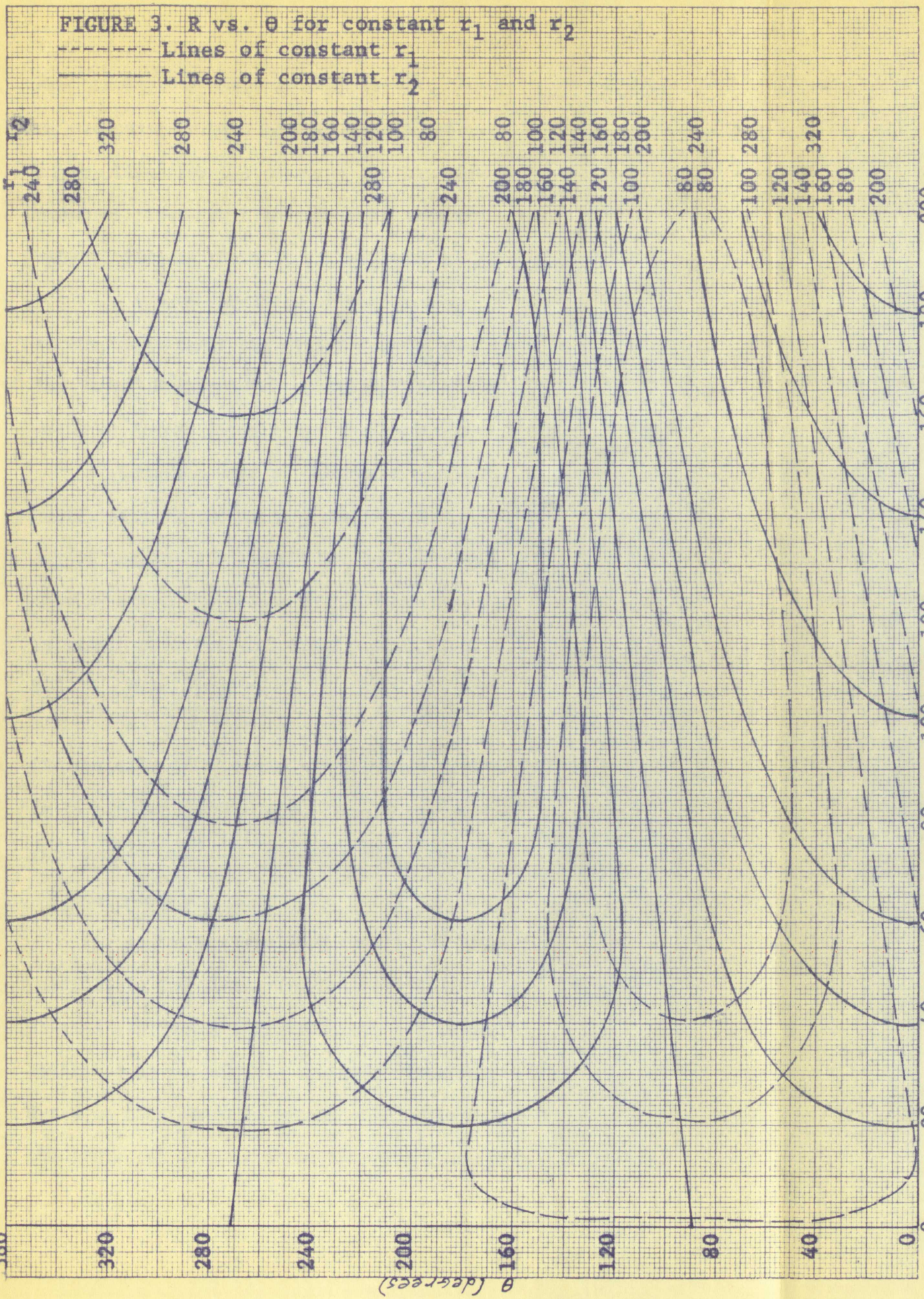
FIGURE 3. R vs. θ for constant r_1 and r_2
Lines of constant r_1
Lines of constant r_2
r_2
320 280 240 200 180 160 140 120 100 80 80 100 120 140 160 180 200 240 280 320
r_1
240 280 280 240 200 180 160 140 120 100 80 80 100 120 140 160 180 200
R (ft)
0 20 40 60 80 100 120 140 160 180 200
θ (degrees)
360 320 280 240 200 160 120 80 40 0

Now choose some value of the ratio A. For each value of x_1 the value of x_2 necessary to give the chosen ratio A can be calculated. The intersection of the lines for the given x_1 and the calculated x_2 can be determined on the graph of figure 3. Thus lines of constant A, and likewise B, can be determined. Some of these lines are shown on the graph in figure 4.

Now the location of the core can be determined. From the readings of the three tanks the ratios A and B can be computed. The intersection of the lines corresponding to the ratios A and B in figure 4 is determined. This point of intersection gives the location of the center of the shower.

Once the core of the shower has been located, the total number of particles N in the shower, can be determined. The distance from the core to any of the small detectors can be found by using the appropriate one of equations 4 or by using the graphs of the type shown in figure 3. From equation 7 it is easily seen that the total number of particles is given by

$$N = \frac{N_1 \, 2\pi r_o^2}{A \, F(x_1)} \qquad (12)$$

The quantity $2\pi r_o^2/AF(x)$ has the same variation with x for all showers. It is plotted in figure 5. Thus N can be computed by multiplying N_1 by the appropriate value of $2\pi r_o^2/A\,F(x_1)$ obtained from the graph in figure 5.

4. Accuracy

As can be seen in figure 4 the lines of constant A become almost parallel to the lines of constant B at a distance of 150 feet and greater. In this region the determination of R is not very good since the error is estimated to be $\pm$10 feet or about $\pm$3 meters. For distances less than 100 feet R can be determined to within $\pm$1.5 feet or about $\pm$0.5 meters. In this region the angle can be determined to an accuracy of $\pm 2^\circ$. Thus for showers whose

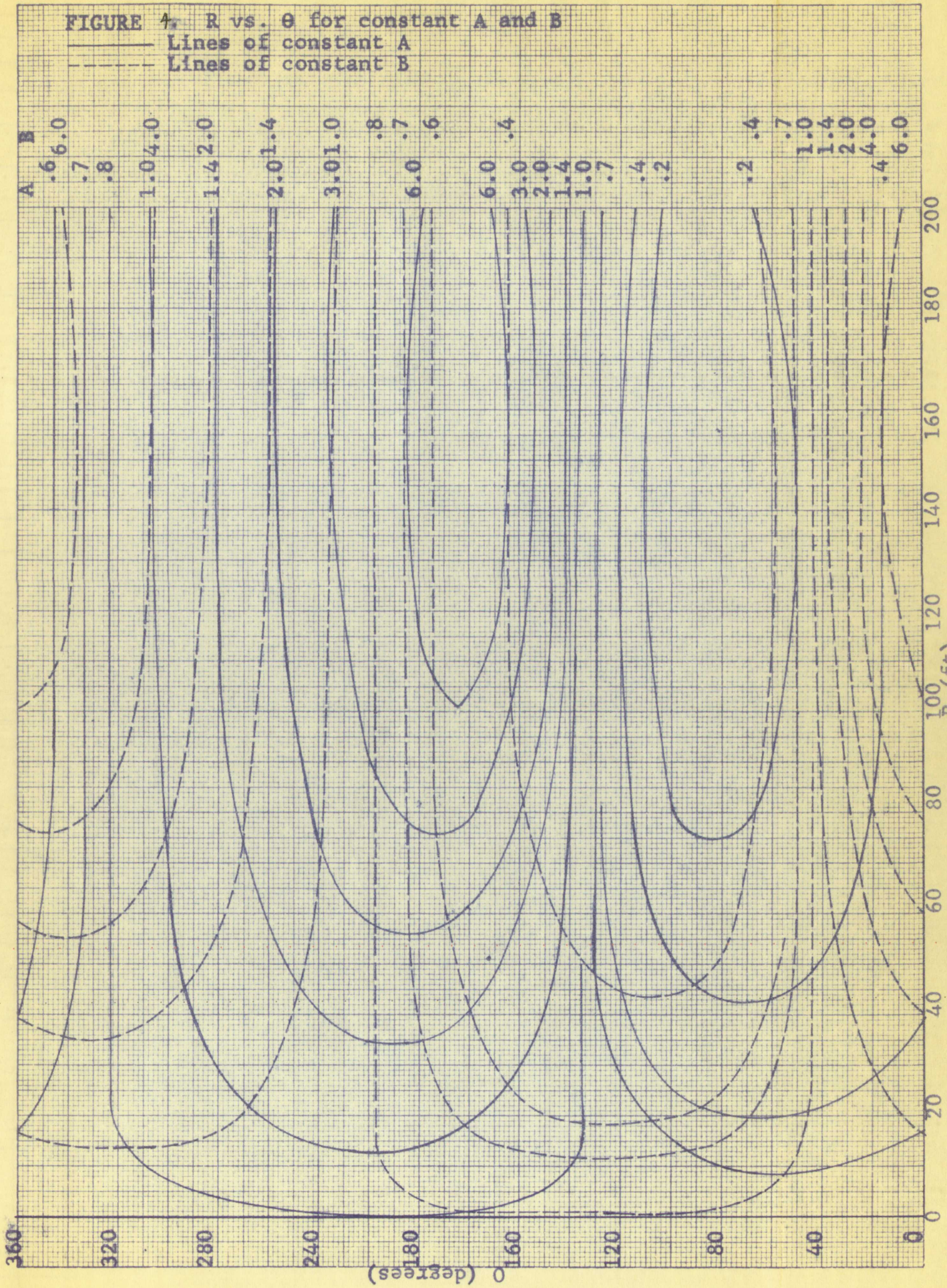
FIGURE 4. R vs. θ for constant A and B
Lines of constant A
Lines of constant B
A B
.6 6.0
.7
.8
1.0 4.0
1.4 2.0
2.0 1.4
3.0 1.0
.8
.7
.6
6.0
.4
6.0
3.0
2.0
1.4
1.0
.7
.4
.2
.2 .4
.7 1.0
1.4 2.0
4.0 6.0
.4
0
20
40
60
80
100
120
140
160
180
200
R (ft)
0
40
80
120
160
200
240
280
320
360
θ (degrees)

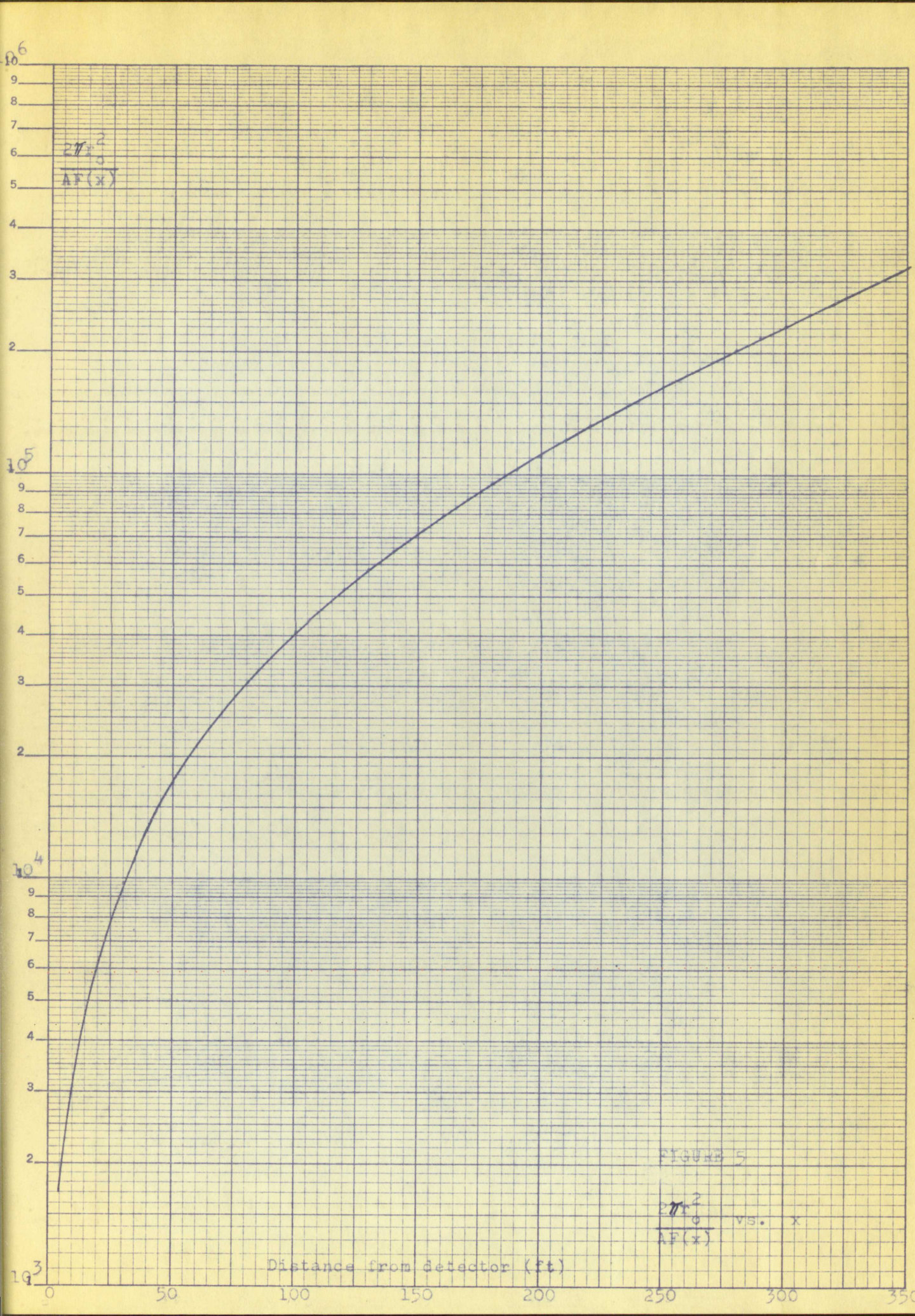

FIGURE 5

$\frac{2\pi r_0^2}{AF(x)}$ vs. x

core is near the large detectors and thus in the region of interest, the location of the core of the shower and hence the site of the shower can be determined quite accurately. The actual results when applied to showers depend on the accuracy of the scintillation detectors in determining the number of particles traversing them.

PART II. RESPONSE OF A SCINTILLATOR TO EXTENSIVE AIR SHOWERS

1. Introduction

Through observations made over the years the spectrum of extensive air showers reaching the surface of the earth is found to be of the form

(13) $R(\geq N) = BN^{-\gamma}$,

where B is a constant. This gives the rate of occurrence of showers of size greater than or equal to N per unit time per unit area regardless of the direction of the axis. If a scintillation detector is used to record the frequency of these showers it will record the number of particles traversing it. It will be shown that the spectrum of particles detected by the scintillator is of the form

(14) $R(\geq p) = Dp^{-\gamma}$,

where D is another constant and the exponent is the same as for the shower size spectrum.

The scintillators in use at the University of New Mexico consist of a liquid scintillator which radiates when a charged particle traverses it. The emitted radiation is usually assumed to be directly proportional to the number of particles traversing the liquid. A photomultiplier tube measures the amount of radiation which is emitted by the scintillation liquid. The construction of the scintillators, along with the associated equipment for handling the output of them, is described in reference 9. The sensitivity of the photomultiplier tube can be varied by varying the supply voltage to the tube. For a given intensity of the radiation from the scintillation liquid, the higher the supply voltage for the tube is the larger the output signal will be. If the tube voltage is too high it will saturate for a low number of particles. In order to be able to record a large number of particles

the tube is operated at a voltage lower than the maximum operating voltage. Thus the range of particles to which the detector is sensitive can be controlled.

Once the range of sensitivity of the detector has been set it is of interest to know the range of shower sizes which, on the average, will give the selected range of particles. Thus a probability function relating p, the number of particles traversing the scintillator, and N, the total number of particles in the shower, is desired. From this function can be calculated the most probable value of N which gives a value of p. Also the average value of N and the average value of N^2 can be determined. All these quantities are of interest so that statements can be made about the range of showers which the scintillator is detecting.

2. Shower Size and Particle Spectra

As was stated earlier the rate at which showers which have more than N particles fall in a unit area per unit time is given by

(15) $$R(\geq N) = BN^{-\gamma}.$$

The differential rate is

(16) $$R(N)dN = K_0 N^{-\gamma-1} dN,$$

where $K_0 = -\gamma B$. This gives the rate at which showers of sizes N to N + dN strike a unit area per unit time.

If we have a scintillation detector of area A, the rate at which showers fall whose axes are at a distance between x and x + dx from the detector and have sizes from N to N + dN is

(17) $$R(x,N)\, d\,x\, dN = K_0 r_4^2 2\pi\, x\, d\, x\, N^{-\gamma-1}\, dN$$

The quantities x and r_4 have been defined earlier (PART I, 2). The number of particles traversing the tank due to a shower of size N to N + dN and

whose axis is a distance between x and x + dx is given by

$$(18) \qquad p = \frac{N A}{r_4^2} f(x) \quad .$$

This equation neglects the variation in particle density over the area of the detector. The distribution function used will be Greisen's approximation to the lateral distribution function of Nishimura and Kamata. It is of the form

$$(19) \qquad f(x) = C(s)\, x^{s-2}\, (x+1)^{s-4.5} \quad .$$

The rate at which p particles traverse the detector due to showers whose core is between the distances x and x + dx from the detector and whose size is between N and N + dN is just the rate given in equation 17, while p is defined by equation 18.

If N is considered fixed and p or more particles are to be recorded by the detector, then the distance of the shower axis from the detector will have to be less than some maximum value. The maximum value is defined by equation 18. To get the rate at which p or more particles are counted due to showers of sizes from N to N + dN, integrate the rate as defined by equation 17 over x from x = 0 to x = x_{max}. The result is

$$(20) \qquad R(\geq p, N)dN = K_o \pi r_4^2 (x_{max})^2 N^{-\gamma-1} dN \quad .$$

By integrating first over N and then over x the following expression can be derived for the integral spectrum of p.[3]

$$(21) \qquad R(\geq p) = \frac{2\pi r_4^2 A^\gamma K_o p^{-\gamma}}{\gamma} \int_o^\infty x\, f^\gamma(x)\, dx$$

The integral over x can be evaluated in terms of Beta functions as[3]

$$(22) \qquad \int_o^\infty x\, f^\gamma(x)\, dx = \frac{C^\gamma(s)}{r_4^{2\gamma}} \frac{\Gamma[(s-2)\gamma + 2] \times \Gamma[(6.5-2s)\gamma - 2]}{\Gamma[\gamma(4.5-s)]} \quad .$$

This is just a function of s and γ. There are restrictions on γ and s so that the integral will converge. When s has the bounds $1 \leq s \leq 1.5$ then γ is restricted according to $0.57 \leq \gamma \leq 2.0$.[3]

If a new variable $z = \frac{NA}{\pi r_4^2}$ is introduced, equation 20 becomes

$$(23) \qquad R(\geq p, z)\, dz = K_o \pi r_4^2 (x_{max})^2 \left[\frac{A}{r_4^2 p}\right]^{\gamma} z^{-\gamma-1}\, dz.$$

When equation 23 is divided by equation 21 the result is a probability distribution function for the new variable z. If W(z) is this probability distribution function then

$$(24) \qquad W(z)\, dz = K (x_{max})^2 z^{-\gamma-1}\, dz,$$

where $K = \frac{\gamma}{2 \cdot C^{\gamma}(s)} \left[\frac{\Gamma[2(4.5-s)]}{\Gamma[(s-2)\gamma + 2]\ \Gamma[(6.5-2s)\gamma - 2]}\right]$.

The maximum value of x was found to be that value of x for which $f(x) = p r_4^2 / NA$. Thus

$$(25) \qquad f(x_{max}) = \frac{1}{z}.$$

To be able to compute W(z) explicitly it is necessary to have a functional form for the inverse of the function f(x); i.e., what is desired is a function g such that

$$(26) \qquad g\left[\frac{1}{z}\right] = x$$

When g has been determined W(z) will have the form

$$(27) \qquad W(z) = K\, g^2\left[\frac{1}{z}\right] z^{-\gamma-1}.$$

Once the inverse function has been determined several quantities involving z may be calculated directly. The most probable value of z

may be determined along with the average value of z and the average value of z^2. Once the average value of z is known, if all other parameters are fixed, the average value of N for a given p can be determined. When the range of particles to which the detector is sensitive is known, the range of shower sizes to which the detector is most sensitive can be determined.

3. Inverse Function

An inverse function is desired for the function

(28) $$f(x) = p\, r_4^2/NA = y.$$

That is, a function g is to be determined so that

(29) $$g(y) = x.$$

The functional form for f(x) is

(30) $$f(x) = C(s)\, x^{s-2}\, (x+1)^{s-4.5}.$$

When this function is plotted, for different values of s, on log-log graph paper the curves are nearly straight lines for large and small values of x. (See reference 7) For small values of x

(31) $$f(x) \simeq C(s)\, x^{s-2},$$

since for small x, $x+1 \simeq 1$. For large values of x

(32) $$f(x) \simeq C(s)\, x^{2s-6.5}$$

since for large x, $x+1 \sim x$. Thus it is reasonable to assume the same general form for the inverse function g(y); i.e., when y is small $g(y) \simeq y^{\gamma}$ and when y is large $g(y) \simeq y^{\alpha+\beta}$. Therefore assumed that g(y) can be written as

(33) $$g(y) = a \left[\frac{y}{b}\right]^{\alpha} \left[\frac{y}{b} + 1\right]^{\beta}$$

where α, β, a and b are constants to be determined.

The constants α and β were determined from the graphs of f(x) published by Nishimura and Kamata[7] and from values computed by Barton.[6]

They are reciprocals of the slopes of the lateral distribution function in the regions where the curves are approximately straight lines on a log-log plot. For small x, or large y, the reciprocal of the slope gives $\alpha + \beta$; for large x, or small y, the reciprocal of the slope gives α. The measured values of α and β are tabulated in Table 2 for several values of β.

TABLE 2
EXPONENTS OF THE INVERSE FUNCTION

s	α	$\alpha + \beta$
.6	-.224	-.716
1.0	-.240	-1.04
1.2	-.262	-1.24
1.4	-.318	-1.87
1.6	-.326	-2.48
2.0	-.48	$-\infty$

Table 2 shows that the values of λ and $\lambda + \beta$ change with the value of s. Therefore it is necessary to express λ and $\lambda + \beta$ as some function of s. It is easy to fit the reciprocals of λ and $\lambda + \beta$ to simple functions of s. The functions

(34) $$\frac{1}{\lambda} = \frac{1}{2}(5-s^{3/2})$$

and $$\frac{1}{\lambda+\beta} = -(2-s)$$

fit the measured values of the reciprocals reasonably well. The calculated values of $\frac{1}{\lambda}$ and $\frac{1}{\lambda+\beta}$ and the measured values are tabulated in Table 3.

They are reciprocals of the slopes of the normal ionization function in the regions where the curves are approximately straight lines on a log-log plot. For small x, or large γ, the reciprocal of the slope gives α. For large x, or small γ, the reciprocal of the slope gives $\alpha+\beta$. The observed values of α and β are tabulated in Table 2 for several values of γ.

TABLE 2

EXPONENTS OF THE IONIZATION FUNCTION

s	α	$\alpha+\beta$
.8	-.284	-.014
1.0	-.240	-.024
1.2	-.202	-.034
1.4	-.168	-.044
1.6	-.138	-.054
2.0	-.93	- ∞

Table 2 shows that the values of α and $\alpha+\beta$ change with the value of s. Therefore it is necessary to express α and $\alpha+\beta$ as some function of s. It is easy to fit the reciprocals of α and $\alpha+\beta$ to simple functions of s. The functions

$$\frac{1}{\alpha} = -(3-s^{3/2}) \tag{34}$$

and

$$\frac{1}{\alpha+\beta} = -(2-s)$$

fit the measured values of the reciprocals reasonably well. The calculated values of $\frac{1}{\alpha}$ and $\frac{1}{\alpha+\beta}$ and the measured values are tabulated in Table 3.

TABLE 3
RECIPROCALS OF THE EXPONENTS FOR THE INVERSE FUNCTION, MEASURED AND CALCULATED

s	$-\frac{1}{\alpha}$		$-\frac{1}{\alpha+\beta}$	
	Measured	Calculated	Measured	Calculated
.6	4.46	4.45	1.398	1.40
1.0	4.06	4.00	.96	1.00
1.2	3.81	3.69	.807	.80
1.4	3.14	3.35	.535	.60
1.6	3.06	2.98	.404	.40

Figures 6 and 7 show the graph of the calculated values and the measured values as functions of s. The maximum percent error between the calculated and measured values for $\frac{1}{\alpha}$ is about 7% and for $\frac{1}{\alpha+\beta}$ it is about 12%. The maximum error occurs for s = 1.4 in both cases. The values of α and β can be found from the following formulas.

(35) $$\alpha = \frac{1}{(s^{3/2}-5)}$$

$$\beta = \frac{1}{(s-2)} + \frac{1}{(5-s^{3/2})}$$

The constants a and b can be determined now. They are found by taking two points on graph (i.e., the distribution function for each value of s) and solving the resultant two simultaneous equations for a and b. The results of this procedure are tabulated in table 4.

TABLE 4
CONSTANTS FOR THE INVERSE FUNCTION

s	a	b
.6	.48	.612
1.0	.61	.622
1.2	.65	.634
1.4	.50	.640

FIGURE 6

$\frac{-1}{\alpha}$ vs. s

—Calculated value

⊙ Measured value

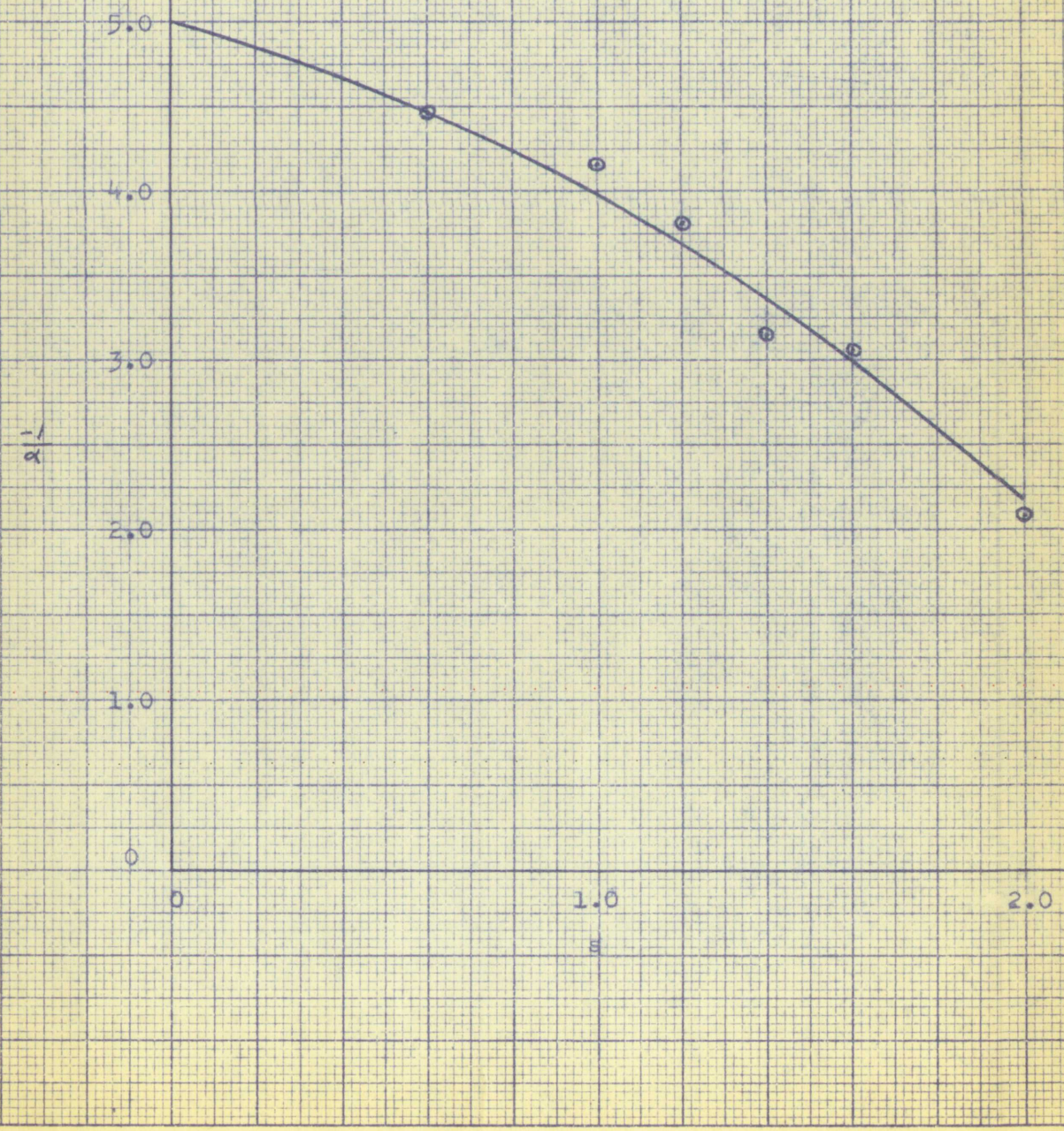

As can be seen in table 4, the values of a and b show no obvious form of variation with s. If there is any true variation with s it is small. Thus an average value is used for a and b in the inverse function. The average values turn out to be

(36) $\bar{a} = .56$

and $\bar{b} = .63.$

The final form of the inverse function is

(37) $$g(y) = (.56) \left|\frac{y}{.63}\right|^{\frac{1}{s^{3/2}-5}} \left|\frac{y}{.63} + 1\right|^{\frac{1}{s-2} + \frac{1}{5-s^{3/2}}}$$

The derived inverse function follows the actual inverse function in general shape. In figures 8, 9, 10 and 11 the solid lines are the inverse functions using Greisen's function.[6] The dashed lines represent the calculated values using the explicit inverse function as derived here. For the range of $g(y) = 10^{-5}$ to $g(y) = 10^{1}$ the best approximate inverse function is therefore $s = 1.4$. This is interesting since the largest error in the exponents, using the measured values as true ones, occurred at $s = 1.4$. For s in the range $1.2 \leq s \leq 1.4$ the inverse function g(y) is a very good approximation to the true inverse function.

4. Use of the Inverse Function

The probability distribution function for z can now be written as

(38) $$w(z) = K' \left[\frac{1}{zb}\right]^{2\alpha + \gamma + 1} \left[\frac{1}{zb} + 1\right]^{2\beta},$$

Where $K' = Kab^{\gamma + 1}$. For a distribution to be meaningful the integral over-all z must be finite. The integral of w(z) can be evaluated by making the substitution $v = \frac{1}{zb}$.

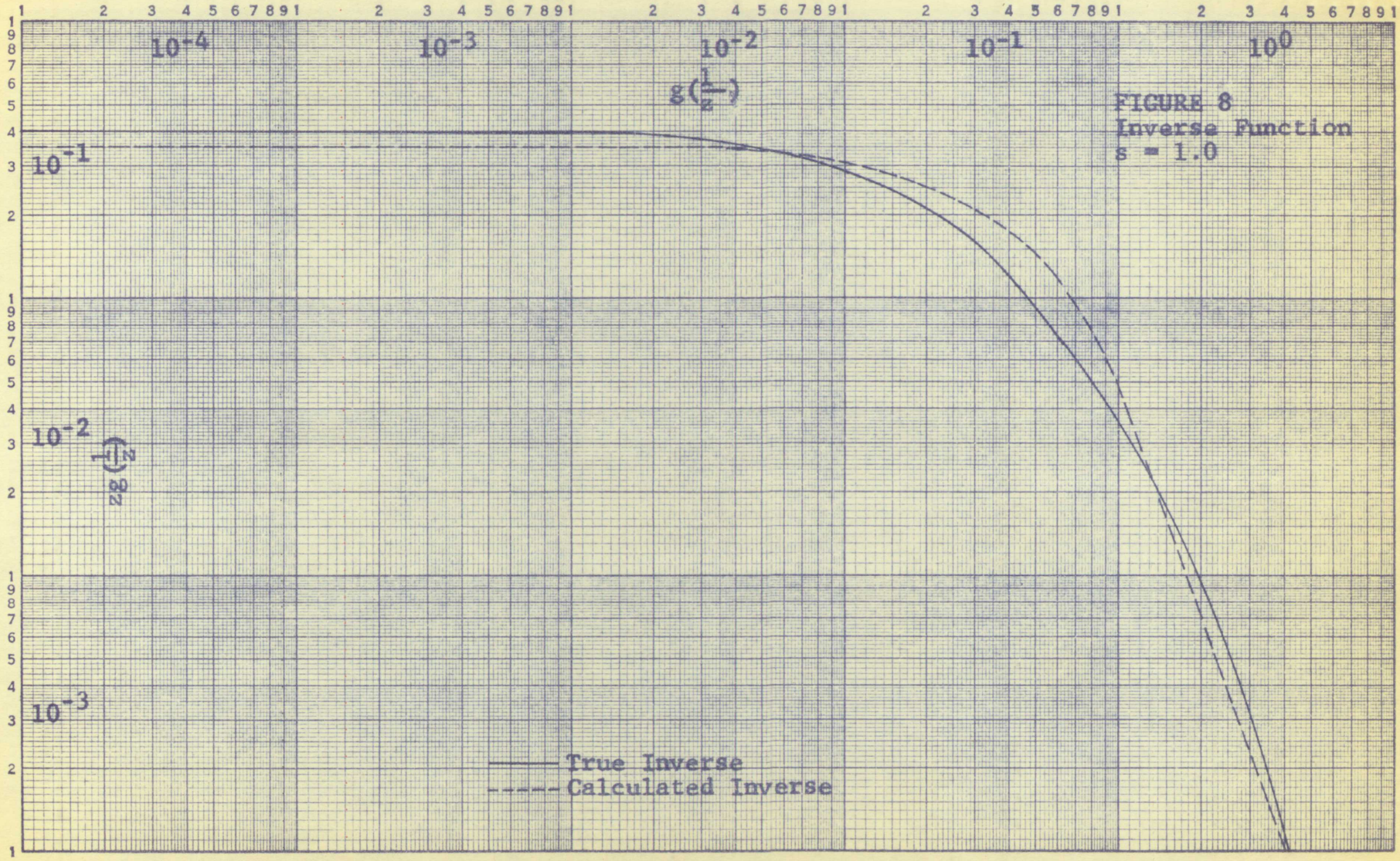

FIGURE 8
Inverse Function
s = 1.0

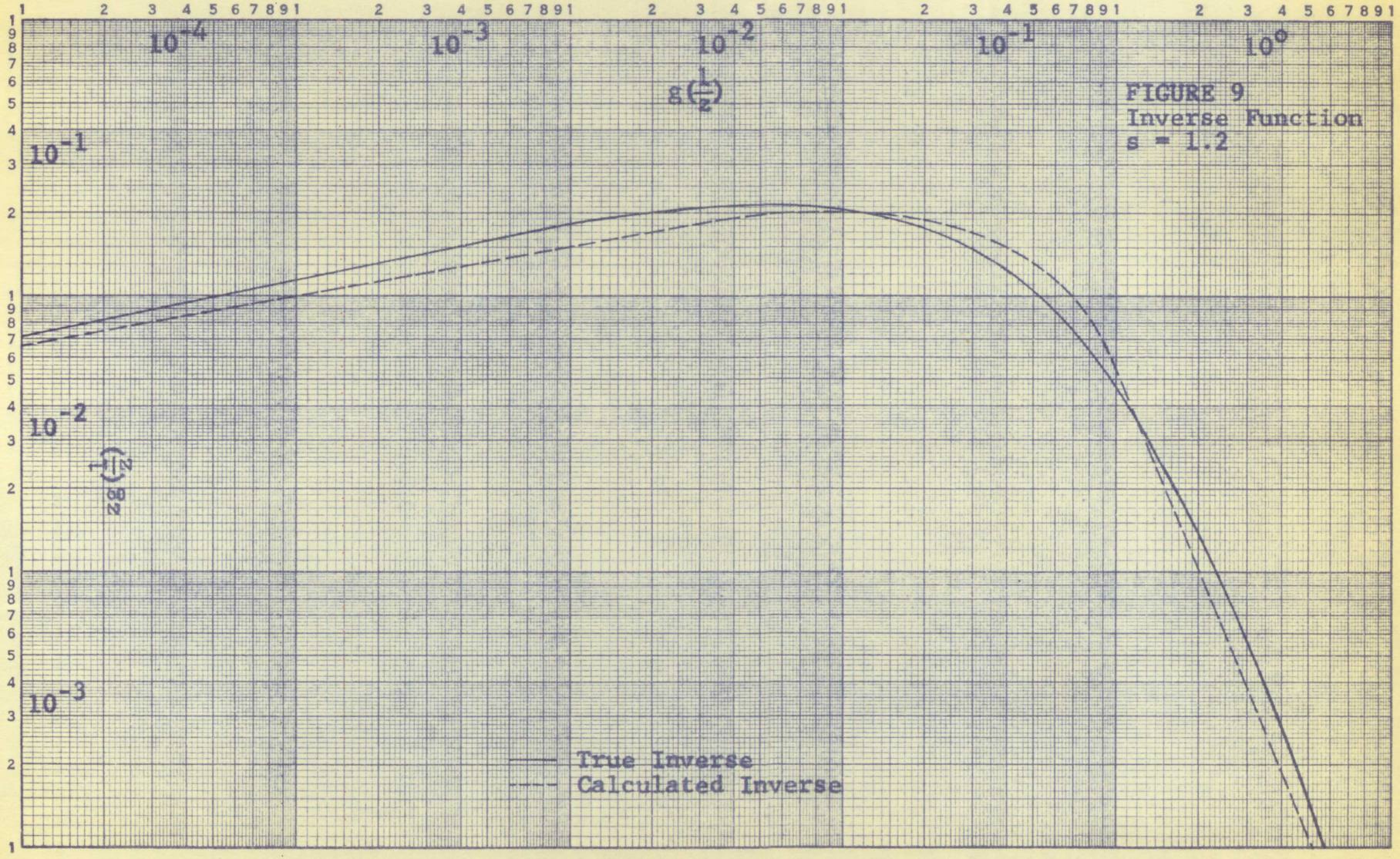

FIGURE 9
Inverse Function
s = 1.2

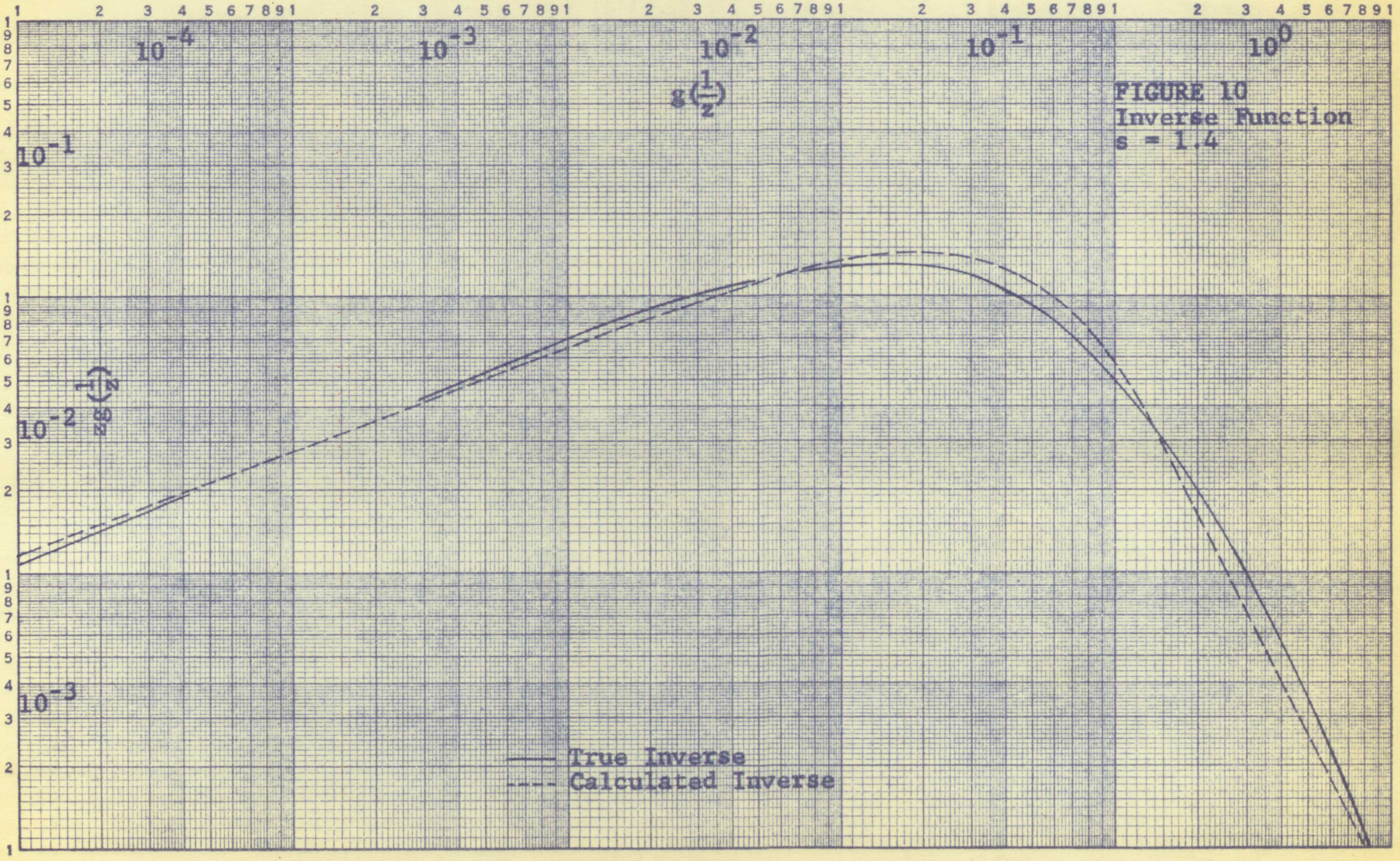

FIGURE 10
Inverse Function
s = 1.4

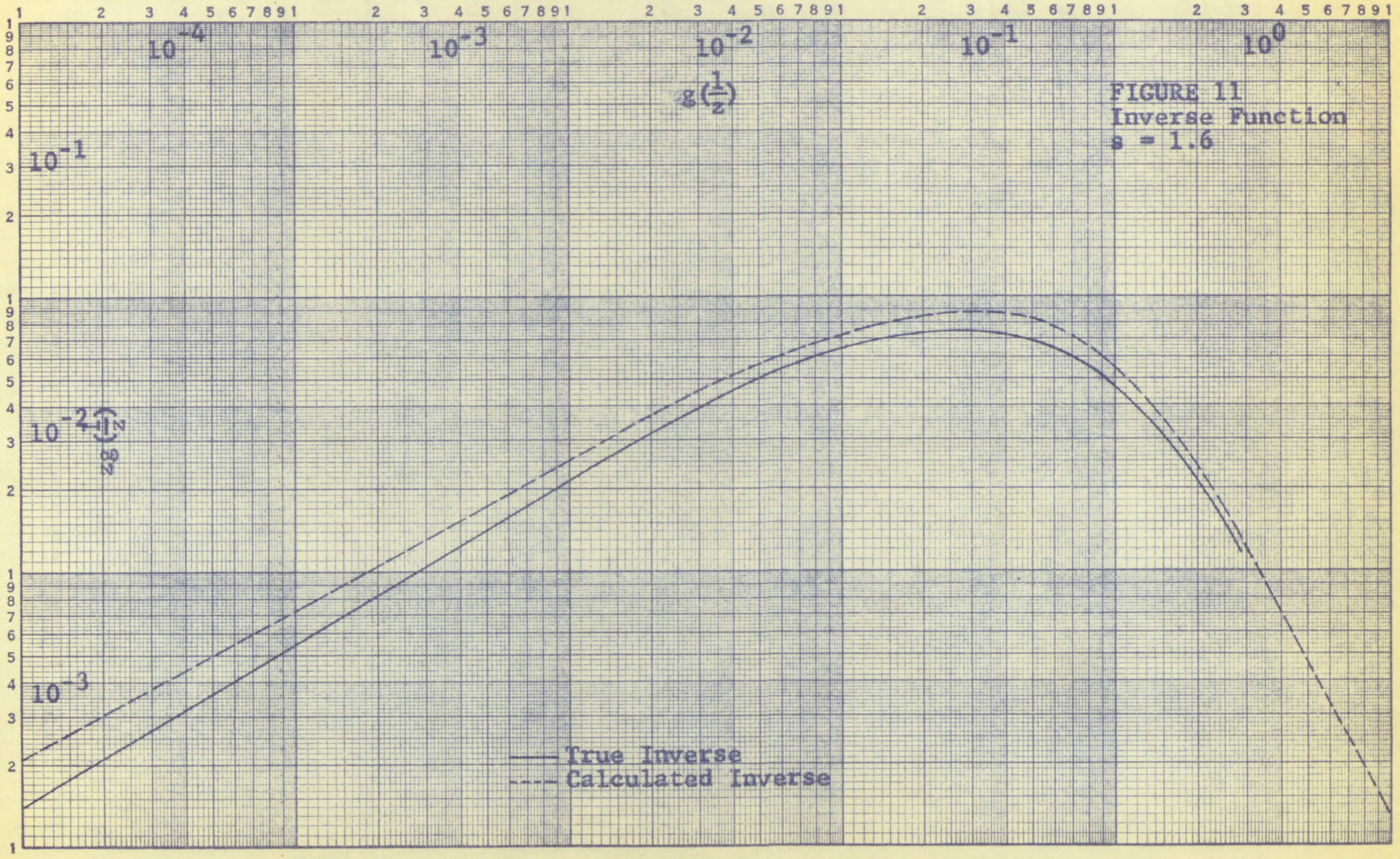

FIGURE 11
Inverse Function
s = 1.6

$$(39) \qquad I = \int_0^\infty w(z)\, dz$$

$$= K' \int_0^\infty \left[\frac{1}{zb}\right]^{2\alpha+\gamma+1} \left[\frac{1}{zb}+1\right]^{2\beta} dz$$

$$= \frac{K'}{b} \int_0^\infty v^{2\alpha+\gamma-1} (v+1)^{2\beta}\, dv$$

This integral can be evaluated in terms of Beta functions.[10]

$$(40) \qquad I = \frac{K'}{b}\, \beta\left[(-2(\alpha+\beta)-\gamma),\ (2\alpha+\gamma)\right] .$$

The normalized form of the distribution function is

$$(41) \qquad W_w(z) = \frac{b}{\beta\left[(-2(\alpha+\beta)-\gamma),\ (2\alpha+\gamma)\right.} \left[\frac{1}{zb}\right]^{2\alpha+\gamma+1} \left[\frac{1}{zb}+1\right]^{2\beta} .$$

For the Beta function to be finite the arguments of the Beta function must be greater than zero. Therefore if the distribution function is to converge, the following inequalities must be satisfied.

$$(42) \qquad -2(\alpha+\beta)-\gamma > 0$$

$$2\alpha+\gamma > 0$$

If the value of γ is taken to be 1.54[11] then the restrictions on α and β become

$$(43) \qquad |\alpha| < .752$$

and $$|\alpha+\beta| > .752$$

From equations 34 the restrictions on s are found to be

$$(44) \qquad .67 < s < 2.4 \quad .$$

The value of s generally used for computations at an elevation of Albuquerque is s = 1.3. This is within the range of values of s for which the distribution function converges.

The distribution function is shown graphically in figure 12. It is plotted for $\gamma = 1.54$ and $s = 1.3$. The scale of w(z) is arbitrary

(30) $$I = \int_0^\infty w(x)\, dx$$

$$= K' \int_0^\infty \left[\frac{1}{2b}\right]^{2\alpha+\gamma+1} \left[\frac{1}{b} - 1\right]^{\beta} dx$$

$$= \frac{B}{K'} \int_0^\infty \frac{2\alpha+\gamma-1}{(\nu+1)^{2\alpha}} \, d\nu$$

This integral can be evaluated in terms of Beta functions.

(40) $$I = \frac{B}{K'} \cdot B\left[-2(\alpha+\beta)-\gamma, (2\alpha+\gamma)\right].$$

The normalized form of the distribution function is

(41) $$M_w(x) = \frac{B\left[(-2(\alpha+\beta)-\gamma, (2\alpha+\gamma+1)\right]}{} \left[\frac{1}{2b}\right]^{2\alpha+\gamma+1} \left[\frac{1}{b} - 1\right]^{\beta}$$

For the Beta function to be finite the arguments of the Beta function must be greater than zero. Therefore if the distribution function is to converge, the following inequalities must be satisfied.

(42) $$-2(\alpha+\beta) - \gamma > 0$$

$$2\alpha + \gamma > 0$$

If the value of γ is taken to be 1.0[11] then the restrictions on α and β become

(43) $$|\alpha| < .707$$

and $$|\alpha+\beta| > .707$$

From equations 34 the restrictions on α are found to be

(44) $$.67 < a < 3.4 .$$

The value of a generally used for computations at an elevation of 10 kilometers is a = 1.3. This is within the range of values of a for which the distribution function converges.

The distribution function is shown graphically in figure 13.

It is plotted for $\beta = 1.34$ and a = 1.3. The scaling of $p(x)$ is arbitrary

and not normalized. As the graph shows, the distribution is spread out over several orders of magnitude. This means that for a given number of particles p in the tank a wide range of shower sizes can be expected to give this value of p. The most probable value of z is that value of z for which the distribution function is a maximum. This occurs at the value of z for which $w'(z) = 0$. Computing the first derivative and setting it equal to zero gives

$$(45) \qquad (2\alpha + \gamma + 1)\left[\frac{1}{zb} + 1\right] + 2\beta\left[\frac{1}{zb}\right] = 0$$

or $$z_{mp} = \frac{2(\alpha+\beta) + \gamma + 1}{b(2\alpha + \gamma + 1)} \quad .$$

From equations 35 the most probable value of z can be written as a function of s and γ as

$$(47) \qquad z_{mp} = -\frac{\left[\frac{s}{s-2} + \gamma\right]}{\left[b\,\frac{s^{3/2} - 3}{s^{3/2} - 5} + \gamma\right]}$$

For $s = 1.3$ and $\gamma = 1.54$ the most probable value of z turns out to be $z = .286$. Since the range of sensitivity of the scintillator is assumed known, an estimation of the range of shower sizes to which the detector is most sensitive can now be given.

The average of z can be computed using the distribution function. It is obtained by evaluating the integral

$$(48) \qquad \bar{z} = \int_0^\infty z w(z)\, dz.$$

This integral can be evaluated in terms of a Beta function in the same way that the integral of equation 39 was evaluated. The arguments of the Beta function are

$$(49) \qquad m = -2(\alpha+\beta) - \gamma + 1$$

and $$n = 2\alpha + \gamma - 1 \quad .$$

and not normalized. As the graph shows, the distribution may vary over several orders of magnitude. This means that for a given number of particles p in the tank a wide range of values may be selected to give this value of p. The most probable value of z is that value of z for which the distribution function is a maximum. This occurs at the value of z for which w'(z) = 0. Computing the first derivative and setting it equal to zero gives

$$(45) \qquad (2\alpha + \gamma + 1)\left[\frac{1}{z_{mp}} + 1\right] + \beta\left[\frac{1}{z_{mp}}\right] = 0$$

or $$z_{mp} = \frac{2(\alpha + \beta) + \gamma + 1}{b(2\alpha + \gamma + 1)} .$$

From equations 35 the most probable value of z can be written as a function of s and δ as

$$(47) \qquad z_{mp} = \left[\frac{s}{\beta - \gamma}\right] \Big/ \left[\frac{s\sqrt{2} - 2}{\beta + \gamma}\right]$$

For s = 1.3 and δ = 1.84 the most probable value of z turns out to be z = .286. Since the range of sensitivity of the oscillator is assumed known, an estimation of the range of power sizes to which the detector is most sensitive can now be given.

The average of z can be computed using the distribution function. It is obtained by evaluating the integral

$$(48) \qquad \bar{z} = \int_0^\infty z w(z)\, dz .$$

This integral can be evaluated in terms of a Beta function in the same way that the integral of equation 39 was evaluated. The arguments of the Beta function are

$$(49) \qquad m = -2(\alpha + \beta) - \gamma + 1$$

and $$n = 2\alpha + \gamma - 1 .$$

If the average value of z is to be finite then both m and n must be postive. Therefore

(50) $$(\alpha + \beta) > \frac{\gamma - 1}{2}$$

and $$(\alpha) < \frac{\gamma - 1}{2}$$

When functional relations for α and β (equations 35) are used and γ is taken to be 1.54 the following restrictions on s are found to be necessary if $\bar{z}$ is to be finite.

(51) $$-1.7 < s < 1.19$$

This seriously restricts the range of s for which $\bar{z}$ is finite. This is just because of the functional form of the inverse function. For s = 1.3 the average value of z is infinite. This is an explanation of why the distribution is so wide as plotted in figure 12.

If the average value of z^2 is computed it is found that it diverges in all cases for $\gamma = 1.54$.

5. Experimental Results

The location and size of 274 showers was determined by the method described in PART I. The experimental details are discussed by J. Moore in reference 12. The top scintillator of the telescope was used as the detector. The value of $\frac{1}{zb}$ was determined for each shower. Then the values of $\frac{1}{zb}$ were broken up into several ranges and the number in each range was counted. Figure 13 shows the results graphically. The maximum occurs between $\frac{1}{zb} = 2 \times 10^{\circ}$ and $\frac{1}{zb} = 4 \times 10^{\circ}$. This is very close to the maximum of the theoretical curve shown in figure 12 where the maximum occurs at $\frac{1}{zb} = 5.5 \times 10^{\circ}$.

FIGURE 12

Theoretical Distribution Function for z

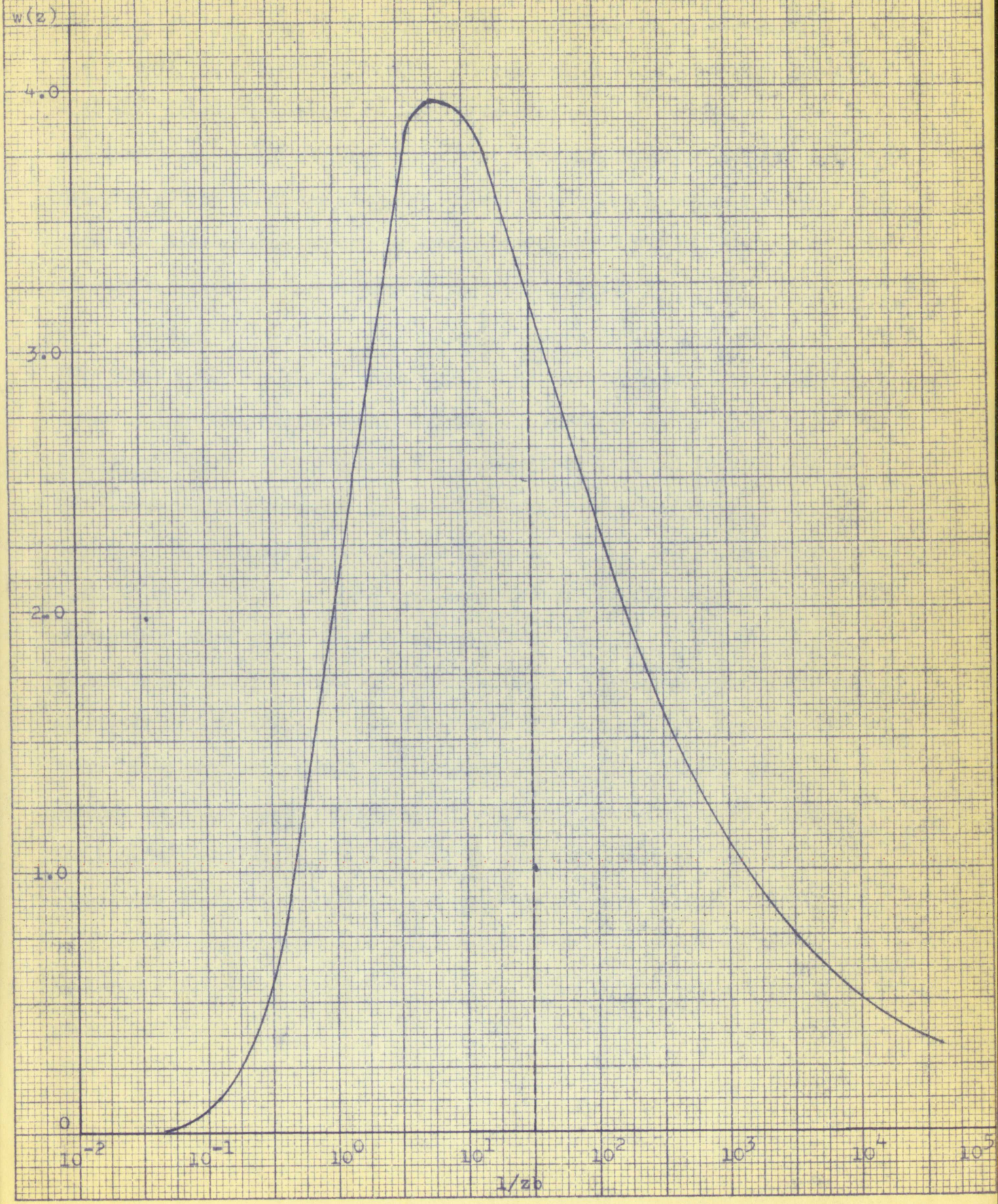

The largest difference between the theoretical and experimental distribution functions is that the experimental curve falls off much faster than the theoretical curve for large values of $\frac{1}{zb}$. When these data were taken, the system was set up so that only large showers near the center tank would be recorded. The system was triggered by the top detector of the telescope when 700 or more particles traversed it. In reference 3 an expression is developed which relates the minimum shower size which will give p particles in the tank. It is

(52) $$N_{min} = 61.2p \ .$$

This gives a minimum shower size of 4.3×10^5 particles to trigger the system. From this the maximum value of $\frac{1}{zb}$ which should occur is $\left[\frac{1}{zb}\right]_{max} = 33.4$. The experimental results bear this out in that only two showers with a value of $\frac{1}{zb}$ greater than the maximum value were detected. Since there is a limit to the range of $\frac{1}{zb}$ the integral of equation 39 should not be from zero to infinity. It should go to the maximum value of v. This would not change the form of the distribution except to introduce the cut-off indicated in the theoretical distribution of Figure 12. It would result in a change of the numerical value of the normalizing constant because the integral corresponding to (39) would produce incomplete Beta functions. The adjusted distribution with cut-off can thus be compared in form with the experimental distribution. The shapes and principal characteristics are seen to agree closely.

The author wishes to thank Professor John R. Green for his assistance in preparing this thesis and Dr. James R. Barcus for helpful discussions.

FIGURE 13

Experimental Distribution Function for z

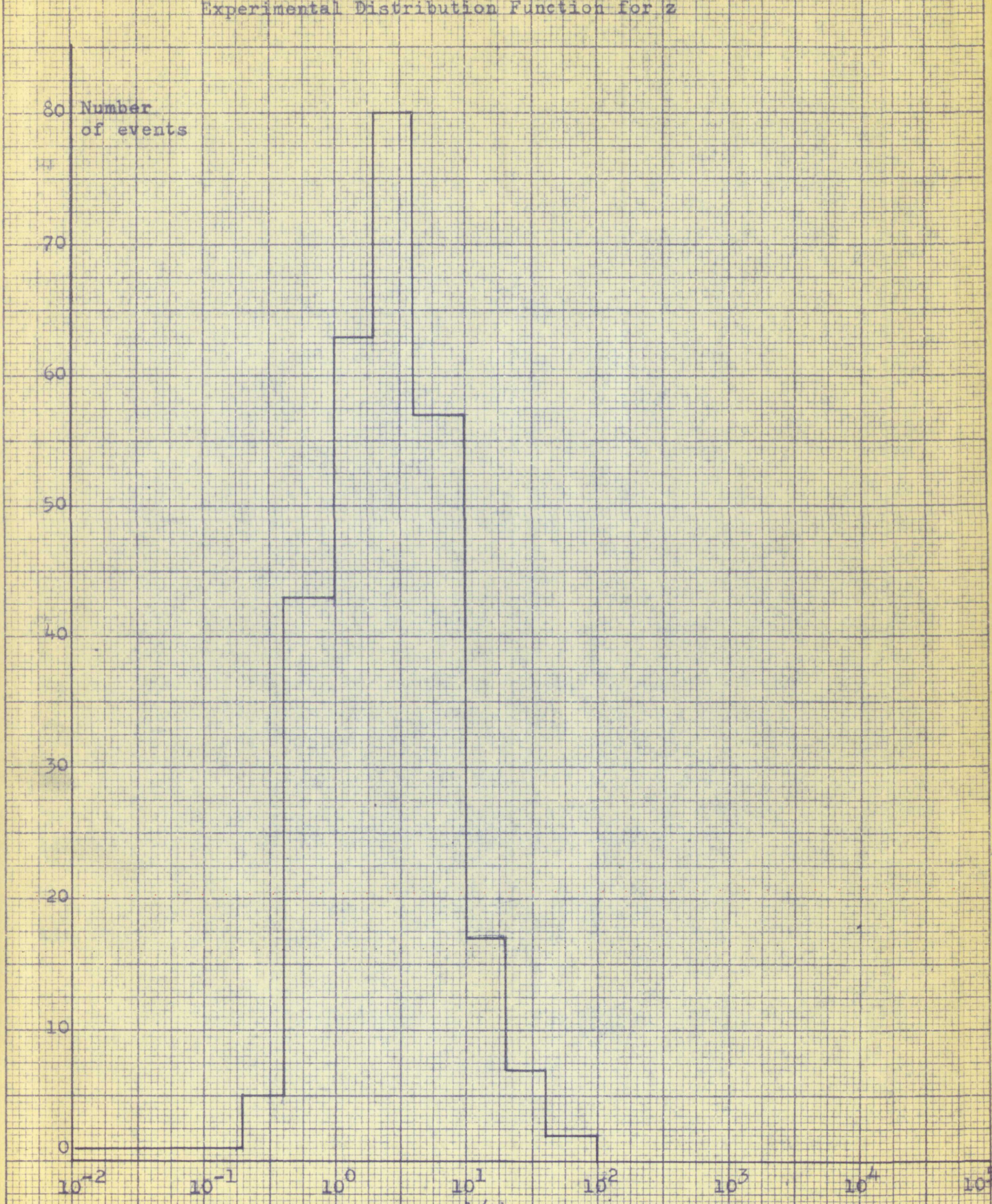

LIST OF REFERENCES

1. Galbraith, William. Extensive Air Showers. New York: Academic Press Inc., 1958

2. Leighton, Robert B. Principles of Modern Physics New York: McGraw-Hill Book Company, Inc., 1959

3. Green, John R. "Size-Spectrum of Extensive Air Showers of the Cosmic Radiation. I-Response of a Single Scintillator to Extensive Air Showers," Il Nuovo Cimento, Vol. 14, 4342, 1959

4. Clark, G., et al. Nature, Vol 180, 353, 1951

5. Greisen, K. Progress in Cosmic Ray Physics, Vol. 3, Chap. 1, 1956

6. Barton, Robert T. "On the Relation Between the Cosmic Ray Air Shower Spectrum and the Pulse Height Spectrum of a Large Scintillator." Masters Thesis, University of New Mexico, 1958

7. Nishimura, J. and Kamata, K. "The Laterial and the Angular Structure Functions of Electron Showers," Supplement of the Progress of Theoretical Physics, No. 6, 93, 1958

8. Green, John R. "Large Scintillator for Observation of Cosmic Rays," Review of Scientific Instruments, Vol. 29, 10, 1958

9. Green, John R. and Barcus, James R. "Size Spectrum of Extensive Air Showers of the Cosmic Radiation," Il Nuovo Cimento, Vol. 14, 1356, 1959

10. Pipes, Louis A. Applied Mathematics for Engineers and Physicists. New York: McGraw-Hill Book Company, Inc., 1958

11. Green, John R. "Extensive Air Showers of the Cosmic Radiation-Final Report," Physics Department, University of New Mexico, 1961. (Mimeographed).

12. Moore, Jerre R. "Experimental Determination of the Distribution of Core Location of Extensive Air Showers." Masters Thesis, University of New Mexico, 1961.

1. Galbraith, William. Extensive Air Showers. New York: Academic Press Inc., 1958.

2. Leighton, Robert B. Principles of Modern Physics. New York: McGraw-Hill Book Company, Inc., 1959.

3. Green, John R. "Size-Spectrum of Extensive Air Showers of the Cosmic Radiation. I--Diagrams of a Simple Scintillator to Extensive Air Showers." Il Nuovo Cimento. Vol. 14, 4342, 1959.

4. Clark, G., et al. Nature, Vol 180, 353, 1957.

5. Greisen, K. Progress in Cosmic Ray Physics. Vol. 3, Chap. 1, 1956.

6. Barton, Robert T. "On the Relation Between the Cosmic Ray Air Shower Spectrum and the Sizes Height Spectrum of a Large Scintillator." Master Thesis, University of New Mexico, 1958.

7. Nishimura, J. and Kamata, K. "The Lateral and the Angular Structure Functions of Electron Showers." Supplement of the Progress of Theoretical Physics, No. 6, 29, 1958.

8. Green, John R. "Large Scintillator for Observation of Cosmic Rays," Review of Scientific Instruments. Vol. 29, 10, 1958.

9. Green, John R. and Barcus, James R. "Size Spectrum of Extensive Air Showers of the Cosmic Radiation." Il Nuovo Cimento. Vol. 14, 1356, 1959.

10. Pipes, Louis A. Applied Mathematics for Engineers and Physicists. New York: McGraw-Hill Book Company, Inc., 1958.

11. Green, John R. "Extensive Air Showers of the Cosmic Radiation-Final Report." Physics Department, University of New Mexico, 1961. (Mimeographed).

12. Moore, Jerre R. "Experimental Determination of the Distribution of Core Location of Extensive Air Showers." Masters Thesis, University of New Mexico, 1961.

IMPORTANT!

Special care should be taken to prevent loss or damage of this volume. If lost or damaged, it must be paid for at the current rate of typing.

Date ~~Loaned~~ Due			
OCT 30 1961	OCT 30 RECD		
DEC 3 1961			
JAN 27 1962			
MAR 1[illegible] 1962			
APR 18 1962			
APR 6 - RECD			
JUN 23 1963			
JUN 8	RECD		